

## Two-Stage Rotation Mechanism for Group-V Precursor Dissociation on Si(001)

Jian-Tao Wang,<sup>1</sup> Changfeng Chen,<sup>2</sup> E. G. Wang,<sup>1</sup> Ding-Sheng Wang,<sup>1</sup> H. Mizuseki,<sup>3</sup> and Y. Kawazoe<sup>3</sup>

<sup>1</sup>Beijing National Laboratory for Condensed Matter Physics, Institute of Physics, Chinese Academy of Sciences, Beijing 100080, China

<sup>2</sup>Department of Physics, University of Nevada, Las Vegas, Nevada 89154, USA

<sup>3</sup>Institute for Materials Research, Tohoku University, Sendai, 980-8577, Japan

(Received 13 March 2006; published 26 July 2006)

We report *ab initio* identification of initial dissociation pathways for Sb<sub>4</sub> and Bi<sub>4</sub> tetramer precursors on Si(001). We reveal a two-stage double piecewise rotation mechanism for the tetramer to ad-dimer conversion involving two distinct pathways: one along the surface dimer row via a rhombus intermediate state and the other across the surface dimer row via a rotated rhombus intermediate state. These two-stage double piecewise rotation processes play a key role in lowering the kinetic barrier by establishing and maintaining energetically favorable bonding between adatoms and substrate atoms. These results provide an excellent account for experimental observations and elucidate their underlying atomistic origin that may offer useful insights for other surface reaction processes.

DOI: 10.1103/PhysRevLett.97.046103

PACS numbers: 68.65.-k, 68.35.Fx, 68.43.Bc, 81.07.-b

The understanding of kinetics and energetics of adatoms and small clusters that diffuse over the Si(001) surface has broad implications for the development of microscopic models for epitaxial growth [1,2] and for the fabrication of nanostructures such as quantum dots and nanowires [3]. In molecular-beam epitaxy, group-V elements (e.g., Sb and Bi) not only play a crucial role in heteroepitaxial crystal growth but also can self-assemble into ordered long ad-dimer lines [4–7]. A key issue for the understanding of these phenomena is a quantitative description of the initial stage dissociation and diffusion of the precursor states towards stable ad-dimer configurations. Scanning tunneling microscopy (STM) measurements reveal predominant Sb<sub>4</sub> [8–10] and Bi<sub>4</sub> [11] tetramer precursor states on Si(001). Similar behavior was observed for Sb adsorbed on a Ge(001) surface [12]. Experimental evidence suggests splitting and rotation of the adsorbed Sb and Bi tetramers on Si(001) [9,13]. On the theoretical side, previous work has studied the rotation of individual group-V ad-dimers on Si(001) [14,15]. However, the more complicated and important initial stage conversion processes of the experimentally observed precursor tetramer states to ad-dimer states have yet to be explored.

In this Letter, we report on a detailed study of the energetics and kinetics of the dissociation processes of Sb and Bi precursor tetramer states on Si(001) using *ab initio* total-energy calculations. We reveal a novel two-stage dissociation mechanism involving double piecewise rotation (DPR) processes that lead to lower kinetic barriers compared to those of direct dissociation pathways. We show that the ball-shaped precursor tetramer cluster from the gas phase adopts two primary adsorption configurations: one perpendicular to ( $T_A$ ) and the other along ( $T_B$ ) the substrate dimer row (see Fig. 1). The  $T_A$  configuration first converts to an intermediate rhombus tetramer perpendicular to the substrate dimer row through a piecewise

rotation process and then dissociates into ad-dimer states through a second piecewise rotation process. Meanwhile, the  $T_B$  configuration can convert into an intermediate rhombus tetramer along the substrate dimer row with a small energy barrier and then further dissociate into the ad-dimer states through a similar double piecewise rotation process. At room temperature or above, configuration  $T_B$  is expected to quickly convert into the rhombus configuration upon adsorption and, thus, elude experimental detection.

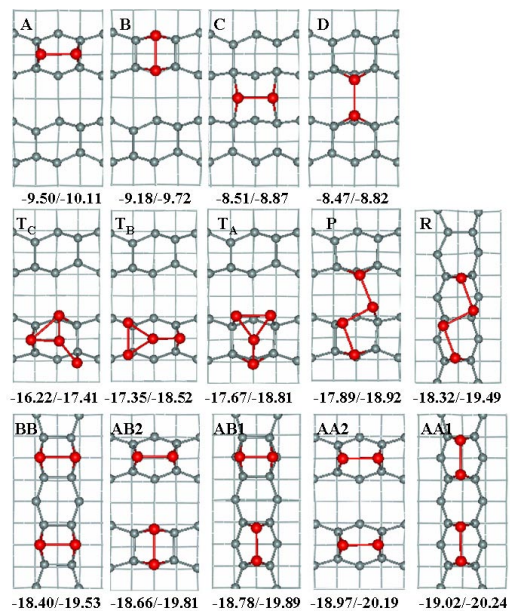


FIG. 1 (color online). Optimized ad-dimer and tetramer configurations and their energies (in eV) defined in the text for Bi/Sb on Si(001). Large (red) and small (gray) circles represent the adatoms and the Si atoms in the top two layers of the substrate, respectively. Lines are drawn to indicate the electronic bonds.

This provides a natural explanation for the absence of the  $T_B$  configuration in STM measurements.

The reported *ab initio* total-energy calculations are carried out using the VASP code [16], employing a plane wave basis set with a 200 eV cutoff energy and the generalized gradient approximation [17]. The electron-ion interaction is described by ultrasoft pseudopotentials [18]. The supercell size is set to  $XYZ = 15.36 \text{ \AA} \times 30.72 \text{ \AA} \times 35.72 \text{ \AA}$  with ten layers of silicon, one layer of hydrogen to passivate the lowest Si layer, and a vacuum layer of about 20 \AA in the  $Z$  direction. In all of the calculations, the top seven layers are fully relaxed while the bottom three are fixed at the bulk structure. The  $XY$  plane corresponds to a  $4 \times 8$  slab with periodic boundary conditions. Forces on the ions are calculated through the Hellmann-Feynman theorem allowing a geometry optimization. The energy minimization is done over the atomic and electronic degrees of freedom using the conjugate gradient iterative technique with two  $k$  points in the  $X$  direction of the Brillouin zone. Many configurations are examined, and the minimum-energy states are used to construct each dissociation and diffusion pathway.

We first calculate the energy of the Bi and Sb ad-dimer and tetramer configurations on Si(001) shown in Fig. 1. These configurations have been considered and some identified in STM experiments for Sb and Bi on Si(001) [8–13]; they also have been identified for Si dimers on Si(001) and Ge dimers on a Ge(001) surface [19]. The energy is defined as  $E_n = E[n] - E[0]$ , where  $E[n]$  and  $E[0]$  are the total energy of the system with and without  $n$  Bi (or Sb) adatoms on the Si(001)- $c(4 \times 2)$  surface, respectively. The calculated results show that the Bi and Sb dimers tend to form on the dimer row, not in the trough between two rows, and the type  $A$  dimer aligned in the direction of the dimer row is the most stable state due to the least induced strain. For  $\text{Sb}_4$  and  $\text{Bi}_4$  on Si(001), the tetramer configurations considered include a rhombus cluster with the long axis along the surface dimer rows ( $R$ ; note that this fully relaxed structure is slightly different from the “dumbbell” structure discussed in Ref. [10]), a rotated rhombus cluster with the long axis perpendicular to the surface dimer rows ( $P$ ), and configurations  $AA$ ,  $AB$ , and  $BB$ , consisting of a pair of loosely coupled type  $A$  and  $B$  dimers in each case. Among them,  $AA$  is the most stable state with the two type  $A$  dimers on the same dimer row ( $AA1$ ) or on two adjacent dimer rows ( $AA2$ ). We also show three ball-shaped tetramers  $T_A$ ,  $T_B$ , and  $T_C$  on the dimer row that resemble the initially adsorbed gas-phase tetrahedral cluster, which have the highest energies among the considered configurations [20]. Our calculated energetic data establish the stability sequence  $T(T_C < T_B < T_A) < P < R \leq BB < AB < AA$  for both Sb and Bi tetramers on Si(001).

Experimentally, for  $\text{Sb}_4$  on Si(001), two different reaction pathways are deduced [10]: one is  $T \rightarrow P \rightarrow AB$  (or  $BB$ ) and the other  $R \rightarrow AB$  (or  $BB$ ). The energy barriers are  $0.7 \pm 0.1$ ,  $0.9 \pm 0.1$ , and  $0.8 \pm 0.1$  eV for  $T \rightarrow P$ ,  $P \rightarrow$

$AB(BB)$ , and  $R \rightarrow AB(BB)$ , respectively. The metastable states  $AB$  or  $BB$  eventually convert to the stable state  $AA$ . There have been no prior study of the mechanisms for the initial stage dissociation of Sb or Bi precursor tetramers on Si(001), which greatly hinders the understanding of these important processes. We report below a systematic examination, using *ab initio* total-energy calculations, of the dissociation pathways. The calculated energy barriers are presented in Table I. We identify the energetically favorable pathways and reveal the key role played by the DPR process in facilitating the structural transformation. We also use the calculated energetic results to resolve the long-standing puzzle that, despite the detection of state  $R$  in STM measurements, its parent tetrahedral cluster state was not observed.

Figure 2 shows the two-stage dissociation pathway across the surface dimer row from  $T_A$  to  $AB2$  via a rotated rhombus ( $P$ ) intermediate state. For the first rotation process from  $T_A$  to  $P$  (path I), at each step we fix the  $x$  ([100]) coordinates of the adatom labeled 4 that moves across the dimer row but allow full relaxation of the  $y$  and  $z$  coordinates. All other adatoms and Si atoms in the top seven layers are also fully relaxed. The rotation process exhibits a rich dynamics of bonding between the adatoms and substrate atoms along the pathway. Initially, the bond between atoms 4–5 is stretched, while a new bond between atoms 2–5 is formed along  $T_A \rightarrow T_{A2}$ . It is followed, along  $T_{A2} \rightarrow P$ , by the sequential breaking of the 4–5 and 2–4 bonds and the simultaneous formation of the 4–7 and 4–8 bonds, completing the first rotation process of ad-dimers 1–2 and 3–4. For the second rotation process from  $P$  to  $AB2$  (path II), at each step we fix the  $x$  ([100]) coordinates of the adatom labeled 3 that moves toward the adjacent dimer row but allow full relaxation of the  $y$  and  $z$  coordinates. Before ad-dimers 3–4 rotate from  $P$  toward  $P_{A2}$ , atom 4 retracts to form the 2–4 bond to reduce the total energy and facilitate the breaking of the 2–3 and 3–6 bonds and the formation of the 3–8 bond, which complete the rotation of ad-dimers 1–2 and 3–4. In comparison, a direct rotation of ad-dimers 3–4 without the 2–4 rebonding would cost an additional 0.19 eV for Sb

TABLE I. Calculated energy barriers (in eV) for (i) the two-stage (first two columns of data) dissociation of Bi and Sb tetramers on Si(001) compared with available experimental (EXP) data for Sb [10], (ii) a direct dissociation pathway (third column), and (iii) the diffusion of the ad-dimers (fourth column).

	$T_A \rightarrow P$	$P \rightarrow AB2$	$T_A \rightarrow AB2$	$B \rightarrow A$
Sb	0.83	0.89	1.47	0.99
Bi	0.71	0.77	1.23	1.03
EXP	$0.7 \pm 0.1$	$0.9 \pm 0.1$		
	$T_B \rightarrow R$	$R \rightarrow AB1$	$T_B \rightarrow AB1$	$B \rightarrow B$
Sb	0.54	0.88	1.06	1.04
Bi	0.49	0.73	0.83	1.08
EXP		$0.8 \pm 0.1$		

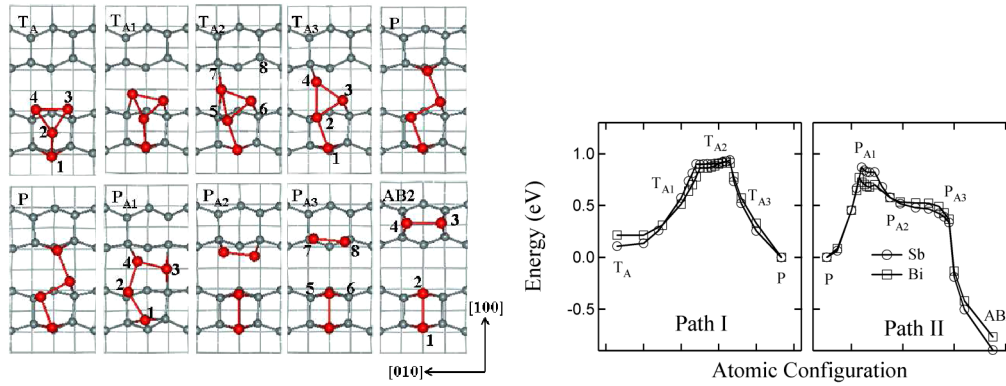


FIG. 2 (color online). The two-stage dissociation pathway and the corresponding energies for  $\text{Sb}_4$  and  $\text{Bi}_4$  on  $\text{Si}(001)$  with the double piecewise rotation process, first from  $T_A$  to  $P$  and then from  $P$  to  $AB2$  across the surface dimer row.

and 0.22 eV for Bi. It shows that rigid-dimer models would be inadequate for such complex rotation processes. Finally, ad-dimers 3–4 move to the most stable  $A$  state with a rolling-over diffusion across the dimer row from  $P_{A2}$  to  $AB$ . During this DPR process across the surface dimer row via the rotated rhombus intermediate state, the energy barriers are estimated to be 0.83 (Sb) and 0.71 eV (Bi) for  $T \rightarrow P$ , and 0.89 (Sb) and 0.77 eV (Bi) for  $P \rightarrow AB$ , respectively, which are in very good agreement with the experimental data of  $0.7 \pm 0.1$  eV for  $T \rightarrow P$  and  $0.9 \pm 0.1$  eV for  $P \rightarrow AB$  as mentioned above.

Figure 3 shows the two-stage dissociation pathway along the surface dimer row from  $T_B$  to  $AB1$  via a rhombus ( $R$ ) intermediate state. It also goes through a similar DPR process with the same computational procedure described above. During the first rotation process (path III), the bond between atoms 4–5 is first stretched and a new bond between atoms 2–5 is formed along  $T_B \rightarrow T_{B2}$ . It is followed, from  $T_{B2}$  toward  $R$ , by the breaking of the bond between atoms 2–4 and the formation of new bonds between atoms 4–7 and 4–8. The energy barriers for this rotation pathway are estimated to be 0.54 eV for Sb and 0.49 eV for Bi. They are clearly lower than the barriers for  $T_A \rightarrow P$  and lead to a much higher rate for the  $T_B \rightarrow R$

conversion. This provides a natural explanation for the puzzling absence of the parent structure of state  $R$  in the STM measurements [10], since at room temperature or above configuration  $T_B$  is expected to quickly convert into the rhombus configuration upon adsorption and, thus, elude experimental detection. Meanwhile, along the second rotation pathway from  $R$  to  $AB$  (path IV), the calculated energy barriers for  $R \rightarrow R_{B1} \rightarrow R_{B2}$  with the rotation of ad-dimers 3–4 are estimated to be 0.88 eV for Sb and 0.73 eV for Bi, which are in very good agreement with the experimental data  $0.8 \pm 0.1$  eV. We note that if ad-dimers 1–2 rotate to the  $A$  state without the intermediate 2–4 bonding associated with the rotation of dimers 3–4 around  $R_{B1}$ , the energy barriers are 1.18 eV for Sb and 1.05 eV for Bi, which are significantly higher than the experimental value. It again shows the intricate dynamic nature of the correlated movements of the adatoms in the conversion process. Finally, ad-dimers 3–4 move to the more stable  $B$  site on the dimer row along the  $R_{B2} \rightarrow AB$  rolling-over diffusion pathway.

For comparison, we also examined pathways with a direct transformation from  $T_A$  to  $AB2$  by moving adatoms 3–4 toward the adjacent dimer row and from  $T_B$  to  $AB1$  by moving adatoms 3–4 along the dimer row. These

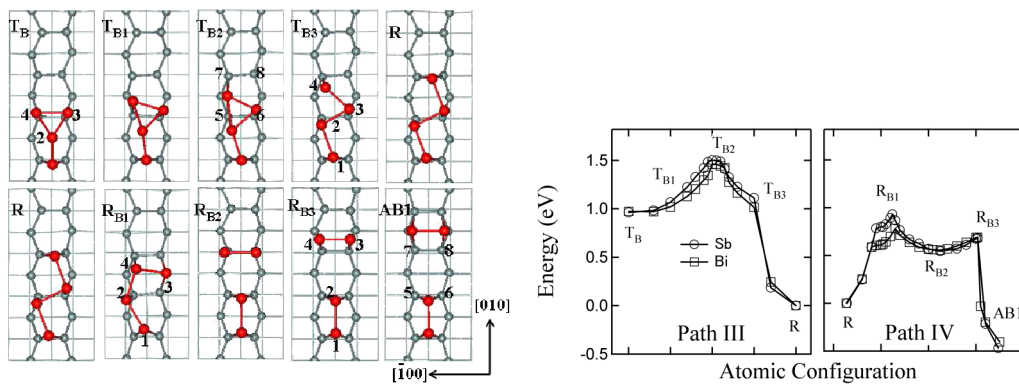


FIG. 3 (color online). The two-stage dissociation pathway and the corresponding energies for  $\text{Sb}_4$  and  $\text{Bi}_4$  on  $\text{Si}(001)$  with the double piecewise rotation process, first from  $T_B$  to  $R$  and then from  $R$  to  $AB1$  along the surface dimer row.



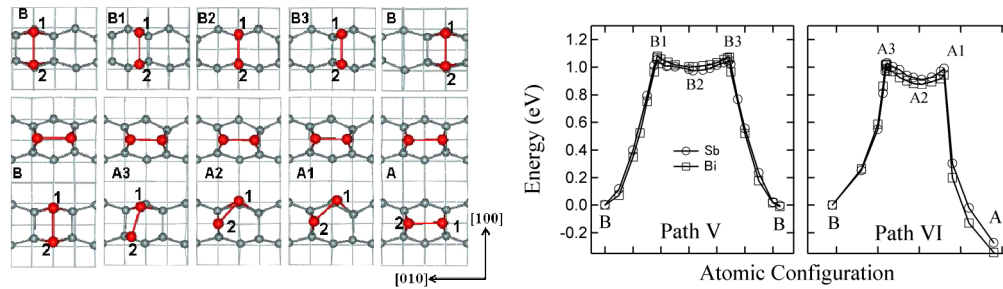


FIG. 4 (color online). The pathways and relative energies for the diffusion of the ad-dimers on Si(001) with a rolling-over process along the surface dimer row from  $B$  to  $B$  and with a piecewise rotation process from  $B$  to  $A$  (or  $AB$  to  $AA$ ).

processes yield energy barriers of 1.47 eV (Sb) for  $T_A \rightarrow AB2$  and 1.06 eV (Sb) for  $T_B \rightarrow AB1$ . These are significantly higher than those for the pathways with the two-stage DPR processes presented above. It is due to the unfavorable bond breaking between adatoms and substrate atoms.

We also studied the conversion of  $BB$  to  $AB$ ,  $AB$  to  $AA$ , and the diffusion of the  $B$  dimer along the dimer row in configuration  $AB$ . We found that the energy barriers for  $BB \rightarrow AB$  and  $AB \rightarrow AA$  are practically the same as that for single dimer diffusion,  $B \rightarrow A$ , reflecting the weak interaction between the  $A$  and  $B$  dimers in the pair. In Fig. 4, path V ( $B \rightarrow B$ ) is a rolling-over pathway along the surface dimer row, and path VI ( $B \rightarrow A$ , or  $AB \rightarrow AA$ ) is a piecewise rotation pathway similar to that reported by Lu *et al.* [21] for the strongly bonded Ge dimers on Si(001). It has one atom rotating at a time instead of more restrictive concerted rigid rotation of both atoms in the dimer. Throughout paths V and VI, there is no Bi-Bi, Sb-Sb, or Si-Si bond breaking. The energy barriers for the diffusion of a type  $B$  dimer along the dimer row are estimated to be 1.08 for Bi and 1.04 eV for Sb dimers, which are very close to the barrier for Si ad-dimer diffusion along the dimer rows, 1.02–1.09 eV/dimer [21]. Meanwhile, those for the dimer rotation from  $B$  to  $A$  (or  $BB \rightarrow AB$ ,  $AB \rightarrow AA$ ) are estimated to be 1.03 for Bi and 0.99 eV for Sb dimers, which are in good agreement with the data reported by Yu *et al.* [14] but lower than 1.28 eV for the concerted rigid rotation pathway [15]. One can see that type  $B$  dimers can easily diffuse along the dimer row or rotate to the most stable type  $A$  state. However, the diffusion and rotation barriers are higher than those for the dissociation, in full agreement with the experimental observation [8–10].

In summary, our detailed *ab initio* total-energy calculations establish a comprehensive understanding of the initial dissociation pathways of Bi and Sb precursor tetramers on Si(001). We reveal a novel two-stage rotation mechanism that optimizes the bonding between the adatoms and the substrate atoms which plays a key role in lowering the kinetic barrier for the structural conversion. The obtained pathways and energy barriers provide a quantitative ac-

count for the experimental observations and a natural explanation for the absence of an initially adsorbed gas-phase tetrahedral cluster in the STM measurements. These results could be extended to the study of surface chemical reaction dynamics important in such processes as chemical vapor deposition and catalysis.

This study was supported by the NSFC, MOST, and MOP of China. C.C. acknowledges support by the U.S. Department of Energy. We are also thankful to the crew of the Center for Computational Materials Science at IMR, Tohoku University for their support at the SR8000 super-computing facilities.

- 
- [1] M. Copel *et al.*, Phys. Rev. Lett. **63**, 632 (1989).
  - [2] I. Hwang *et al.*, Phys. Rev. Lett. **80**, 4229 (1998).
  - [3] M. Kawamura *et al.*, Phys. Rev. Lett. **91**, 096102 (2003).
  - [4] J. H. G. Owen *et al.*, Phys. Rev. Lett. **88**, 226104 (2002).
  - [5] J. H. G. Owen *et al.*, Surf. Sci. **527**, L177 (2003).
  - [6] J. T. Wang *et al.*, Phys. Rev. B **67**, 193307 (2003); Phys. Rev. Lett. **94**, 226103 (2005).
  - [7] O. Kubo *et al.*, Appl. Surf. Sci. **169–170**, 93 (2001).
  - [8] Y. W. Mo, Phys. Rev. Lett. **69**, 3643 (1992).
  - [9] Y. W. Mo, Science **261**, 886 (1993).
  - [10] Y. W. Mo, Phys. Rev. B **48**, 17 233 (1993).
  - [11] M. Naitoh *et al.*, Surf. Sci. **377–379**, 899 (1997); **482–485**, 1440 (2001).
  - [12] L. H. Chan *et al.*, Phys. Rev. B **63**, 195309 (2001).
  - [13] S. Yu. Bulavenko *et al.*, Surf. Sci. **482–485**, 370 (2001); **507–510**, 119 (2002).
  - [14] B. D. Yu and A. Oshiyama, Phys. Rev. B **50**, 8942 (1994).
  - [15] K. Chuasiripattana and G. P. Srivastava, Phys. Rev. B **71**, 153312 (2005).
  - [16] G. Kresse *et al.*, Comput. Mater. Sci. **6**, 15 (1996).
  - [17] J. P. Perdew *et al.*, Phys. Rev. B **45**, 13 244 (1992).
  - [18] D. Vanderbilt, Phys. Rev. B **41**, 7892 (1990).
  - [19] H. J. W. Zandvliet *et al.*, Phys. Rev. Lett. **84**, 1523 (2000).
  - [20] Among the tetrahedral structures,  $T_A$  is the most stable and  $T_C$  is the most unstable which can rotate to  $T_A$  or  $T_B$  with no energy barrier. Meanwhile, the rotation from  $T_B$  to  $T_A$  would encounter an energy barrier of 1.2 eV.
  - [21] Z. Y. Lu *et al.*, Phys. Rev. B **62**, 8104 (2000); Phys. Rev. Lett. **85**, 5603 (2000).